AMERICAN SOCIETY FOR MICROBIOLOGY | mBio®

RESEARCH ARTICLE

In Vivo Competitions between *Fibrobacter succinogenes*, *Ruminococcus flavefaciens*, and *Ruminoccus albus* in a Gnotobiotic Sheep Model Revealed by Multi-Omic Analyses

Carl J. Yeoman,[a] Christopher J. Fields,[b] Pascale Lepercq,[c] Philippe Ruiz,[d] Evelyne Forano,[d] Bryan A. White,[e,f] Pascale Mosoni[d]

[a]Department of Animal and Range Sciences, Montana State University, Bozeman, Montana, USA
[b]Biotechnology Center, University of Illinois at Urbana-Champaign, Urbana, Illinois, USA
[c]TBI, Université de Toulouse, CNRS, INRAE, INSA, Toulouse, France
[d]Université Clermont Auvergne, INRAE, UMR 454 MEDIS, Clermont-Ferrand, France
[e]Carl R. Woese Institute for Genomic Biology, University of Illinois at Urbana-Champaign, Urbana, Illinois, USA
[f]Department of Animal Sciences, University of Illinois, Urbana, Illinois, USA

ABSTRACT *Fibrobacter succinogenes*, *Ruminococcus albus*, and *Ruminococcus flavefaciens* are the three predominant cellulolytic bacterial species found in the rumen. *In vitro* studies have shown that these species compete for adherence to, and growth upon, cellulosic biomass. Yet their molecular interactions *in vivo* have not heretofore been examined. Gnotobiotically raised lambs harboring a 17-h-old immature microbiota devoid of culturable cellulolytic bacteria and methanogens were inoculated first with *F. succinogenes* S85 and *Methanobrevibacter* sp. strain 87.7, and 5 months later, the lambs were inoculated with *R. albus* 8 and *R. flavefaciens* FD-1. Longitudinal samples were collected and profiled for population dynamics, gene expression, fibrolytic enzyme activity, *in sacco* fibrolysis, and metabolite profiling. Quantitative PCR, metagenome and metatranscriptome data show that *F. succinogenes* establishes at high levels initially but is gradually outcompeted following the introduction of the ruminococci. This shift resulted in an increase in carboxymethyl cellulase (CMCase) and xylanase activities but not in greater fibrolysis, suggesting that *F. succinogenes* and ruminococci deploy different but equally effective means to degrade plant cell walls. Expression profiles showed that *F. succinogenes* relied upon outer membrane vesicles and a diverse repertoire of CAZymes, while *R. albus* and *R. flavefaciens* preferred type IV pili and either CBM37-harboring or cellulosomal carbohydrate-active enzymes (CAZymes), respectively. The changes in cellulolytics also affected the rumen metabolome, including an increase in acetate and butyrate at the expense of propionate. In conclusion, this study provides the first demonstration of *in vivo* competition between the three predominant cellulolytic bacteria and provides insight on the influence of these ecological interactions on rumen fibrolytic function and metabolomic response.

IMPORTANCE Ruminant animals, including cattle and sheep, depend on their rumen microbiota to digest plant biomass and convert it into absorbable energy. Considering that the extent of meat and milk production depends on the efficiency of the microbiota to deconstruct plant cell walls, the functionality of predominant rumen cellulolytic bacteria, *Fibrobacter succinogenes*, *Ruminococcus albus*, and *Ruminococcus flavefaciens*, has been extensively studied *in vitro* to obtain a better knowledge of how they operate to hydrolyze polysaccharides and ultimately find ways to enhance animal production. This study provides the first evidence of *in vivo* competitions between *F. succinogenes* and the two *Ruminococcus* species. It shows that a simple disequilibrium within the cellulolytic community has repercussions on the rumen metabolome and fermentation end

Citation Yeoman CJ, Fields CJ, Lepercq P, Ruiz P, Forano E, White BA, Mosoni P. 2021. *In vivo* competitions between *Fibrobacter succinogenes*, *Ruminococcus flavefaciens*, and *Ruminoccus albus* in a gnotobiotic sheep model revealed by multi-omic analyses. mBio 12:e03533-20. https://doi.org/10.1128/mBio.03533-20.

Copyright © 2021 Yeoman et al. This is an open-access article distributed under the terms of the Creative Commons Attribution 4.0 International license.

Address correspondence to Pascale Mosoni, pascale.mosoni@inrae.fr.

This article is a direct contribution from Bryan A. White, a Fellow of the American Academy of Microbiology, who arranged for and secured reviews by Gregory Siragusa, Scout Microbiology LLC, and Stephen Lindemann, Purdue University.

Received 15 December 2020
Accepted 4 January 2021
Published 3 March 2021

Downloaded from https://journals.asm.org/journal/mbio on 08 September 2022 by 153.90.170.56.

products. This finding will have to be considered in the future when determining strategies aiming at directing rumen fermentations for animal production.

KEYWORDS pili IV, CAZymes, cellulose degradation, gnotobiotic animal model, outer membrane vesicles, rumen

Cellulose typically represents ~40% of plant biomass (1) but is not endogenously degradable by mammalian species, including ruminants, due to a lack of an endogenously encoded ability to hydrolyze this important carbohydrate resource. Mammals are instead dependent on members of their gastrointestinal tract microbiota for providing this capability (2). Ruminant animals, including cattle and sheep, harbor a core rumen microbiome (3), including a limited number of taxa known to specialize in the deconstruction of cellulose (4, 5). The three best described and cultivable cellulolytic bacteria, *Fibrobacter succinogenes*, *Ruminococcus albus*, and *Ruminococcus flavefaciens*, each employ unique methods of fulfilling this function. *R. flavefaciens* facilitates cellulose deconstruction by virtue of a cellulosome (6); *R. albus* instead appears to utilize noncellulosomal, but coalescing membrane-attached enzymes (7), while the organization of the cellulolytic system of *F. succinogenes* remains enigmatic, with outer membrane vesicles (OMVs) possibly involved (8, 9). Each of these species is frequently detected among a variety of adult ruminants throughout the world and often cooccur in the rumen (3, 4). Previous *in vitro* studies have provided evidence of competition among these cellulolytic species for adhesion to plant biomass and for growth on cellulose substrates (10–12). However, little is known about their symbiotic relationships *in vivo* or the antagonistic or synergistic impact of their cooccurrence on fibrolysis. We sought to determine how the three species interact molecularly *in vivo* within a previously described and tractable gnotobiotic sheep model (13, 14) and to evaluate how variations in their composition affect ruminal fibrolysis and metabolism alongside a methanogenic hydrogenotroph.

RESULTS

***Fibrobacter succinogenes* is outcompeted following inoculation of ruminococci.** *Fibrobacter succinogenes* S85 (week 3), *Methanobrevibacter* sp. strain 87.7 (week 7), *Ruminococcus albus* 8, and *R. flavefaciens* FD1 (week 28) were sequentially inoculated into two gnotobiotic lambs that were raised aseptically from birth to 37 weeks (Fig. 1). Microbial composition dynamics were monitored from weeks 22 to 33 using quantitative PCR (qPCR) (Fig. 2) and most probable number (MPN) enumeration of total cultivable and total cultivable cellulolytic bacteria (see Fig. S1 in the supplemental material). Using qPCR, the total number of bacteria observed throughout the sampling period showed little variation at $10^{10.3 \pm 0.16}$ 16S rDNA copies/g of rumen content (Fig. 2). These numbers did not vary between the two animals ($P = 0.5$) and were consistent with those measured by MPN ($10^{10.2 \pm 0.4}$ cells/ml) (Fig. S1A and S1B). qPCR data indicated that *F. succinogenes* was initially dominant, being enumerated at $10^{9.4 \pm 0.25}$ 16S rDNA copies/g prior to inoculation of the two *Ruminococcus* strains. Following inoculation with the two *Ruminococcus* strains, *F. succinogenes* was gradually outcompeted in both animals. By week 33, *R. albus* and *R. flavefaciens* were enumerated at $10^{8.8 \pm 0.2}$ and $10^{5.9 \pm 0.4}$ 16S rDNA copies/g, respectively, while *F. succinogenes* was enumerated at $10^{4.7 \pm 0.8}$ 16S rDNA copies/g (Fig. 2). *Methanobrevibacter* sp. 87.7 was enumerated at $10^{5.8 \pm 0.9}$ 16S rDNA copies/g, and total cultivable methanogens were enumerated by MPN at $10^{6.2 \pm 1.01}$ cells/ml throughout the sampling period and exhibited noticeable fluctuation over the first 3 weeks following inoculation of the *Ruminococcus* spp. (Fig. S1C). Consistent with both qPCR and MPN data, most metagenomic and metatranscriptomic reads aligned to the *F. succinogenes* S85 reference genome at week 27 with only low to modest alignment to the *Methanobrevibacter* sp. 87.7 and the two *Ruminococcus* genomes (Fig. S2A). *F. succinogenes* was also well represented in metagenomic, but not metatranscriptomic, data from weeks 29 and 31 and obtained almost no coverage by week 33. This transition, was also seen in the increasing alignment of

Downloaded from https://journals.asm.org/journal/mbio on 08 September 2022 by 153.90.170.56.

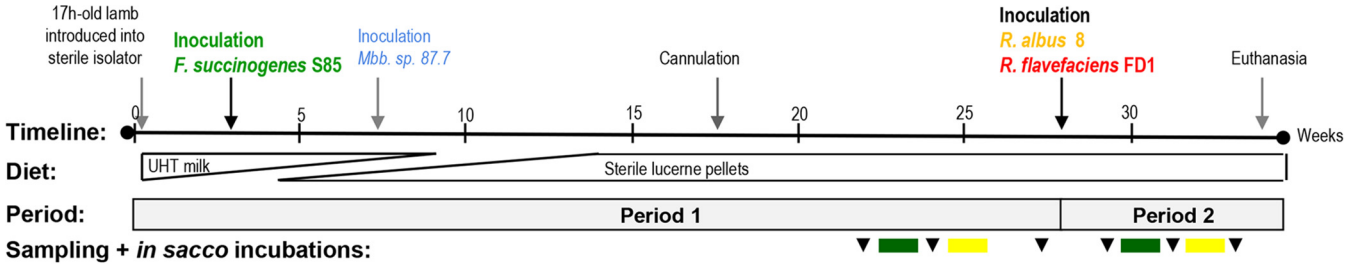


FIG 1 Overview of animal trial. The lambs were initially fed sterilized cow milk (until weaning at week 14) and then sterilized lucerne hay pellets. They were inoculated with *F. succinogenes* S85 (week 3), *Methanobrevibacter* (*Mbb.*) sp. 87.7 (week 7), and *R. albus* 8 and *R. flavefaciens* FD1 (week 28). Periods 1 and 2 correspond to pre- and postinoculation of the ruminococci, respectively. Sampling of rumen contents during both periods are indicated by black triangles. *In sacco* incubations of lucerne and wheat straw cell walls are indicated by green and yellow rectangles, respectively.

these data to the *R. albus* and *R. flavefaciens* genomes between weeks 29 and 33 (Fig. S2A).

Gene expression. Carbohydrate-active enzymes (CAZymes) and accessory systems putatively involved in bacterial adhesion or polysaccharide utilization represented 11%, 21%, and 25% of the total transcriptomes of *F. succinogenes*, *R. albus*, and *R. flavefaciens*, respectively (Fig. 3), while *Methanobrevibacter* sp. 87.7 expressed mostly genes involved in methanogenesis and redox systems (on average 5.5% of total gene expression) (Fig. 3). The expression of CAZymes by each cellulolytic species reflected each bacterium's relative abundance in each sample (Fig. S2A and S2B). Although the inoculated cellulolytic strains each encoded approximately 100 CAZyme genes (see http://www.cazy.org/), only a small subset of those genes were expressed at >1% of their total CAZy gene expression (Fig. 4; see Table S1 in the supplemental material). The 15 most highly expressed CAZyme genes from each of the three cellulolytic strains across all time points were genes targeting cellulose (glycoside hydrolase 5 [GH5], GH8, GH9, GH48, and GH51), hemicelluloses (GH10, GH11, GH26, GH43, and carbohydrate esterase 4 [CE4]) and pectins (polysaccharide lyase 11 [PL11] and CE12). Notably, each of *R. albus*' and *R. flavefaciens*' 15 most expressed CAZyme transcripts encoded proteins harboring either a family 37 carbohydrate-binding module or a dockerin, respectively (Fig. 4). A more diverse carbohydrate transport and metabolism gene expression profile was measured when the ecosystem harbored high numbers of *F. succinogenes* S85 (period 1) compared to that observed following the introduction of the ruminococci (period 2) (Fig. 5). *R. albus* and *R. flavefaciens* were observed to most abundantly

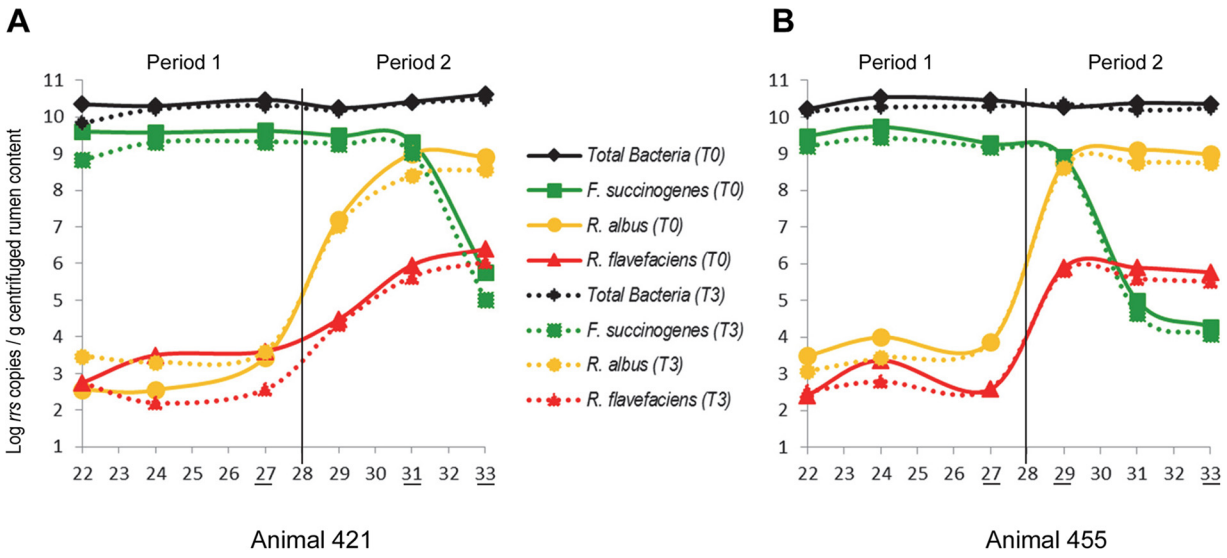


FIG 2 Dynamics of total bacteria and *F. succinogenes*, *R. albus*, and *R. flavefaciens*. The numbers of 16S copies/gram of rumen material evaluated by quantitative PCR in rumen contents pre- and postinoculation of the ruminococci (at week 28) are shown.

Downloaded from https://journals.asm.org/journal/mbio on 08 September 2022 by 153.90.170.56.

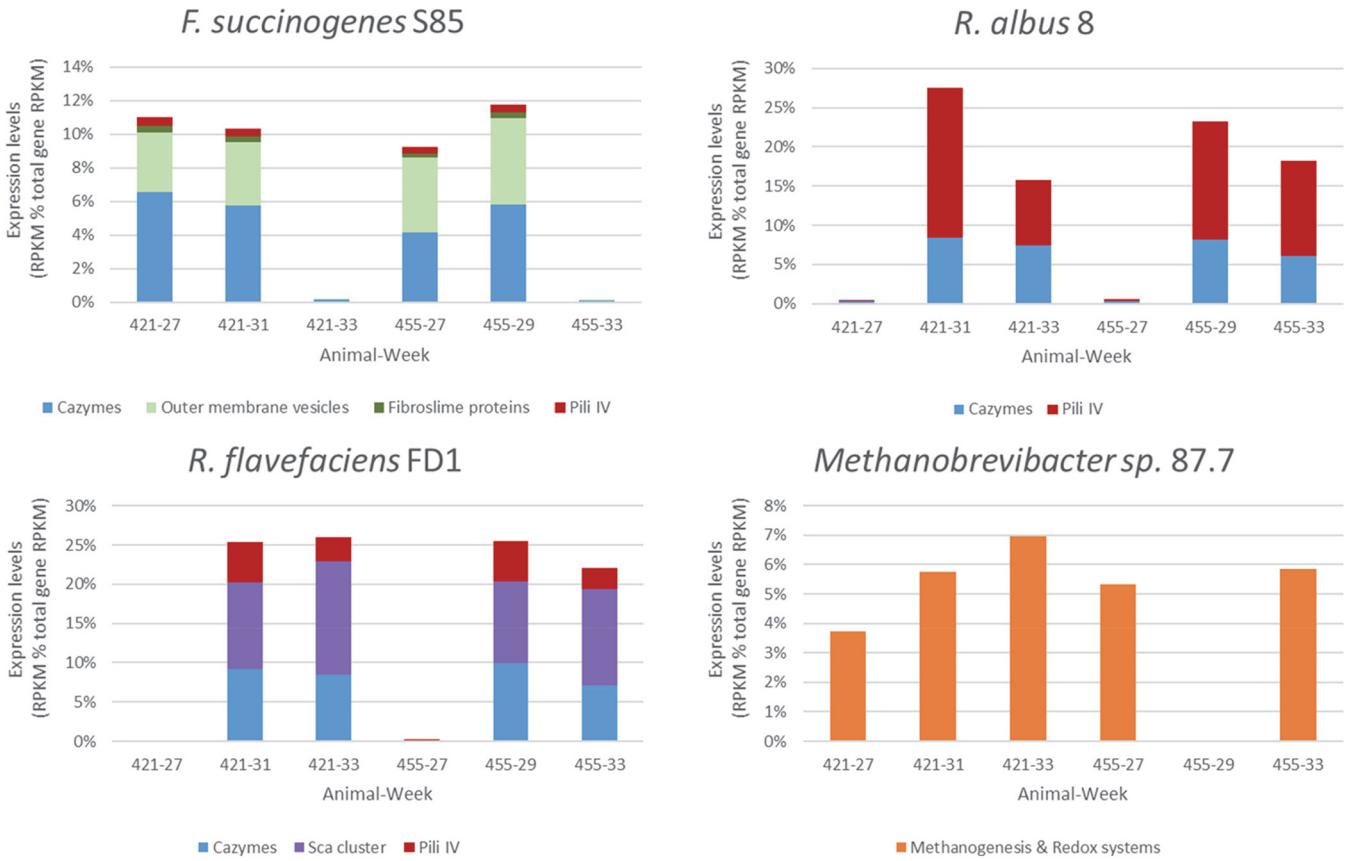


FIG 3 Major functional or structural genes expressed by the four inoculated strains *in vivo*. Relevant functional or structural genes expressed by *F. succinogenes* S85, *R. albus* 8, *R. flavefaciens* FD-1, and *Methanobrevibacter* 87.7 are given in Table S1 in the supplemental material, in addition to the calculations of the percentages of each group of expressed genes within each genome. These percentages were used to generate the four histograms presented here.

express GH9 and GH48 family mRNAs and their inoculation resulted in a dramatic increase in the level of these transcripts that corresponded to decreases in GH2 and GH43 mRNAs (Fig. 5). In addition to CAZymes, *F. succinogenes* exhibited high expression of genes predicted to be involved in the production of extracellular structures, including outer membrane vesicles (OMVs) (4% of total expression). *R. albus* 8 expressed type IV pilus genes (14% of total gene expression), and *R. flavefaciens* FD1 expressed both cellulosomal and type IV pilus genes (12 and 4% of total expression, respectively) (Table S1). Fibro-slime domain containing genes mostly exhibited only low to moderate expression by *F. succinogenes* (0.35% of total gene expression), the exception being FSU_RS11870 (FSU_2502) that was expressed at ~1,000 reads per kilobase per million (RPKM) initially prior to the introduction of the ruminococci (Table S1).

Adhesion to plant biomass. Using qPCR, we further sought to determine any preferential binding of the three inoculated cellulolytic organisms to plant biomass. The distribution of the three species adherent to cannula-inserted *in sacco* samples of either lucerne (alfalfa) or wheat straw reflected their measured abundances in the rumen content with no obvious preference of each cellulolytic species to one or other substrate (Fig. S3). Consistently, scanning electron microscopy (SEM) analyses of both substrates revealed high densities of adherent rod morphotypes consistent with *F. succinogenes*' cell morphology (Fig. S4) prior to the inoculation of the two cellulolytic ruminococci. After inoculation of *R. albus* and *R. flavefaciens*, adherent cocci were observed consistent with the *Ruminococcus* cell morphology (Fig. S4). *F. succinogenes*-like morphotypes remained evident in these later samples although they were never observed alongside *Ruminococcus*-like morphotypes, suggesting spatial partitioning.

Downloaded from https://journals.asm.org/journal/mbio on 08 September 2022 by 153.90.170.56.

***Fibrobacter succinogenes* S85**

locus_tag	421 wk27	421 wk31	421 wk33	455 wk27	455 wk29	455 wk33	protein_id	dbCAN hits	Complementary annotation
FSU_RS10935	2323	621	0	3127	911	0	WP_015732116.1	GH8(0.99)	endoglucanase (Fisuc_1802;FSU_2303)
FSU_RS01825	2004	660	0	3084	914	0	WP_014545209.1	CBM11(0.99),GH51(0.60)	endoglucanase 2 / F (Eg2;CelF;EgF;CBP-4;Fisuc_3111;FSU_0382)
FSU_RS09555	1565	462	0	2863	707	0	WP_014546211.1	CBM11(0.79)	Fisuc_1525 / FSU_2007
FSU_RS00775	1102	410	0	1971	541	0	WP_014545007.1	GH94(0.75)	Fisuc_2900 / FSU_0162
FSU_RS09580	1391	463	0	1432	659	0	WP_014546216.1	GH18(0.94)	Fisuc_1530 / FSU_2012 (CBP-9)
FSU_RS05835	1534	323	0	1369	206	0	WP_014545546.1	GH5(0.87)	Fisuc_0786 / FSU_1228
FSU_RS13850	944	291	0	1498	462	0	WP_014546992.1	GH5(0.87)	cellulase (Fisuc_2364;FSU_2914)
FSU_RS07970	979	265	0	1168	256	0	WP_015731951.1	GH8(0.97)	Fisuc_1219 / FSU_1680 or FSU_1681 ???
FSU_RS07990	862	281	0	969	417	1	WP_014545944.1	GH5(0.98)	Fisuc_1224 / FSU_1685
FSU_RS05545	1154	308	0	729	261	0	WP_015731802.1	GH5(0.83)	Fisuc_0728 / FSU_1166
FSU_RS11205	829	307	0	941	358	0	WP_014546520.1	GH9(0.99)	endoglucanase 1 (CelE;End1;Fisuc_1859;FSU_2361)
FSU_RS05540	1209	130	0	877	62	0	WP_014545497.1	CBM35(0.98),GH26(0.99)	Fisuc_0727 / FSU_1165
FSU_RS12040	705	368	0	848	352	0	WP_014546666.1	GH5(0.83)	Fisuc_2011 / FSU_2534
FSU_RS03685	491	379	0	411	903	0	WP_012820204.1	GH11(0.98)	xylanase C (XynC;Fisuc_0362;FSU_0777)
FSU_RS12485	881	136	0	812	143	0	WP_014546747.1	GT35(1.00)	Fisuc_2097 / FSU_2626 (GlgP)

***Ruminococcus albus* 8**

locus_tag	421 wk27	421 wk31	421 wk33	455 wk27	455 wk29	455 wk33	protein_id	dbCAN hits	Complementary annotation
CUS_RS17265	0	11318	9701	0	8573	12447	WP_002853199.1	CBM37(0.98),CBM4(0.98),GH9(0.99)	Cel9B
CUS_RS06185	0	8443	9157	0	7482	9240	WP_002848405.1	CBM37(0.97),GH48(1.00)	Cel48A
CUS_RS14100	0	1518	1089	1	3698	4017	WP_002851899.1	CBM37(0.98)	
CUS_RS15355	0	1819	2377	0	892	3081	WP_002852491.1	CBM37(0.98)	
CUS_RS15645	0	2035	2368	0	1336	1976	WP_002852384.1	CBM37(0.98),CBM65(0.72),GH5(0.80)	
CUS_RS13150	0	886	840	0	2420	2464	WP_002851506.1	CBM37(0.95)	
CUS_RS18405	0	954	1460	0	1322	2132	WP_002846972.1	dockerin(0.57)	
CUS_RS18470	0	977	792	0	1731	2271	WP_002847476.1	dockerin(0.71)	
CUS_RS10005	0	1264	1301	0	712	910	WP_002850130.1	CBM37(0.97),GH5(0.86)	
CUS_RS11380	0	1016	1049	0	804	801	WP_002850840.1	CBM37(0.98),GH9(1.00)	
CUS_RS17270	0	965	1221	0	560	723	WP_002853289.1	CBM3(0.83),CBM37(0.97),GH9(1.00)	
CUS_RS18435	0	699	972	0	363	680	WP_002847376.1	CBM22(0.96),CBM37(0.97),GH11(0.99)	
CUS_RS11900	0	385	583	0	588	997	WP_037277242.1	GT2(0.35)	
CUS_RS18840	0	579	762	0	257	449	WP_050792249.1	CBM22(0.97),CBM37(0.97),CE4(0.84),GH11(0.99)	
CUS_RS04555	0	390	489	0	479	660	WP_002847919.1	GH130(0.99)	

***Ruminococcus flavefaciens* FD1**

locus_tag	421 wk27	421 wk31	421 wk33	455 wk27	455 wk29	455 wk33	protein_id	dbCAN hits	Complementary annotation
RUMFLAFD1_RS0105550	0	2924	5367	0	3100	1463	WP_009984152.1	CBM30(0.92),CBM4(0.97),GH9(0.99)	dockerin
RUMFLAFD1_RS23820	0	2749	4345	0	2713	1195	WP_009987706.1	GH48(1.00)	dockerin
RUMFLAFD1_RS0120100	0	1299	5943	0	447	487	WP_009987923.1	dockerin(0.90)	dockerin
RUMFLAFD1_RS22520	0	1336	2912	0	1417	822	WP_009985073.1	CBM13(0.79),PL11(0.97)	dockerin
RUMFLAFD1_RS0115725	0	864	2133	0	769	779	WP_009986801.1	CBM13(0.82),CBM35(0.94),CE12(1.00)	dockerin
RUMFLAFD1_RS24095	0	676	1205	0	820	358	WP_009982648.1	GH25(0.99)	
RUMFLAFD1_RS24515	0	645	685	0	643	187	WP_009984389.1	CBM79(0.98),GH9(1.00)	dockerin
RUMFLAFD1_RS0114025	0	443	969	0	309	263	WP_009986298.1	CBM80(0.99),GH5(0.79)	dockerin
RUMFLAFD1_RS25070	0	358	473	0	355	150	WP_009987773.1	GH5(0.87)	dockerin
RUMFLAFD1_RS24530	0	321	487	0	293	196	WP_009984467.1	CBM80(0.89),GH5(0.87)	dockerin
RUMFLAFD1_RS24470	0	163	519	0	99	159	WP_009984269.1	CBM22(0.98),CE4(0.89),GH10(0.96),GH11(0.99),GH124(0.30)	dockerin
RUMFLAFD1_RS0105545	0	212	380	0	179	109	WP_009984151.1	CBM3(0.88),GH9(1.00)	dockerin
RUMFLAFD1_RS0118855	1	139	337	1	168	90	WP_009987608.1	GH94(0.74)	
RUMFLAFD1_RS0118900	0	162	268	0	208	92	WP_009987618.1	CBM22(0.96),GH10(0.99),GH43(0.98)	dockerin
RUMFLAFD1_RS0112325	0	173	296	0	95	96	WP_009985868.1	CBM35(0.84),GH26(1.00)	dockerin

Heatmap Legend

Min = 0 RPKM

Max = 1000 RPKM

FIG 4 Top 15 CAZy gene expression levels by the three inoculated cellulolytic strains *in vivo*. The 15 most abundant CAZyme transcripts of each cellulolytic strain were retrieved from Table S1. CAZyme transcripts of *F. succinogenes* S85, *R. albus* 8, and *R. flavefaciens* FD-1 were sorted

(Continued on next page)

Downloaded from https://journals.asm.org/journal/mbio on 08 September 2022 by 153.90.170.56.

Fibrolytic activity. Zymogram profiles revealed carboxymethyl cellulase (CMCase) and xylanase enzyme profiles to be consistent with those of a pure culture of *F. succinogenes* initially at week 27 but to be more similar to pure *R. albus* and *R. flavefaciens* culture profiles at week 33 (Fig. 6). Total rumen CMCase and xylanase specific activity increased 2.6-fold during this same period (Table 1). However, increases in these fibrolytic activities were not reflected by *in sacco* experiments, where no significant increase was seen in the rates of dry matter (DM), neutral detergent fiber (NDF), or acid detergent fiber (ADF) disappearance of either lucerne or wheat straw ($P > 0.05$) (Table 2).

Rumen metabolomics. The rumen metabolome (Table S2) varied by animal and sample day (Fig. 7A and B). Profiles obtained before (week [wk] 27 [initial]) and immediately following the addition of the ruminococci (wk 30 [transitory]) revealed five discriminant metabolites that included a decrease in the free sugar's glucopyranose and galactofuranose and the cellulose-derived keto acid levulinic acid (Fig. 7C). As the ruminococci outcompeted *F. succinogenes* (wk 30 versus wk 33 [final]), 11 discriminant metabolites were observed, including decreases in ferulic acid and increases in several phenolic metabolites (Fig. 7D). Comparisons of initial and final time points revealed nine discriminant metabolites (Fig. 7E), including an increase in 3-(3-hydroxyphenyl) propionic acid and a decrease in oxalic acid. Targeted metabolomic analyses of fermentation end products revealed that acetate and butyrate increased in their relative abundance following establishment of the ruminococci at the expense of propionate (Fig. S5).

DISCUSSION

The functional ecology of the major cellulolytic bacteria of the rumen was studied for the first time *in vivo* within a tractable animal model using complementary molecular, microbiological, enzymatic, and nutritional techniques. The animal model harbored in its rumen an immature microbiota that was limited to those microbes acquired during the first 17 h of contact with the mother (see Text S1 in the supplemental material). The lack of cultivable cellulolytic and methanogenic communities and measurable activities in our animal model allowed us to control the cellulolytic and methanogenic populations in a sequential manner by inoculating specific strains harboring these functions and then observe competition among three major rumen cellulolytic species. Multiple analyses revealed that *R. albus* became numerically, transcriptionally, and enzymatically dominant within 4 weeks of inoculation. This observation agrees with several *in vitro* coculture experiments that have also shown that *R. albus* was the most competitive in initial adhesion to, and growth, on cellulose (10, 12, 15). The high adherence of *R. albus* has been described *in vitro* to be the result of cell-surface-located type IV pili (16–18), CBM37-containing glycoside hydrolases (19, 20), and a glycocalyx (21). We observed high expression of type IV pilus genes by both *R. albus* and *R. flavefaciens* supporting an important role for these extracellular appendages in adhesion to cellulose *in vivo* (16–18, 22). Our data also support the importance of CBM37-harboring CAZymes by *R. albus* and cellulosome by *R. flavefaciens* for fiber breakdown *in vivo* with GH9 and GH48 family enzymes appearing to be preferred for ruminococcal cellulolytic function (7, 19, 20, 22).

R. albus has also been shown to produce *in vitro* a bacteriocin active against *R. flavefaciens* but not against *F. succinogenes* (23, 24). The gene encoding this bacteriocin in *R. albus* 8 has been described (25), and we found that it is very poorly transcribed in our animal model whatever the period (data not shown). Hence, bacteriocin production by *R. albus* cannot explain the fact that *R. flavefaciens* did not establish at high levels. *R. flavefaciens* was, however, able to numerically outcompete *F. succinogenes*.

FIG 4 Legend (Continued)
in Table S1 from the highest to lowest expression counts (expressed in RPKM) using the sum of counts of each transcript in the two animals (421 and 455) at the three sampling times. For each gene, the encoded protein identifier (ID) is given along with its modular composition (dbCAN hits) and complementary annotation provided on the CAZy site (http://www.cazy.org/) or determined by manual annotation using BLASTP on NCBI (https://blast.ncbi.nlm.nih.gov/Blast.cgi).

Downloaded from https://journals.asm.org/journal/mbio on 08 September 2022 by 153.90.170.56.

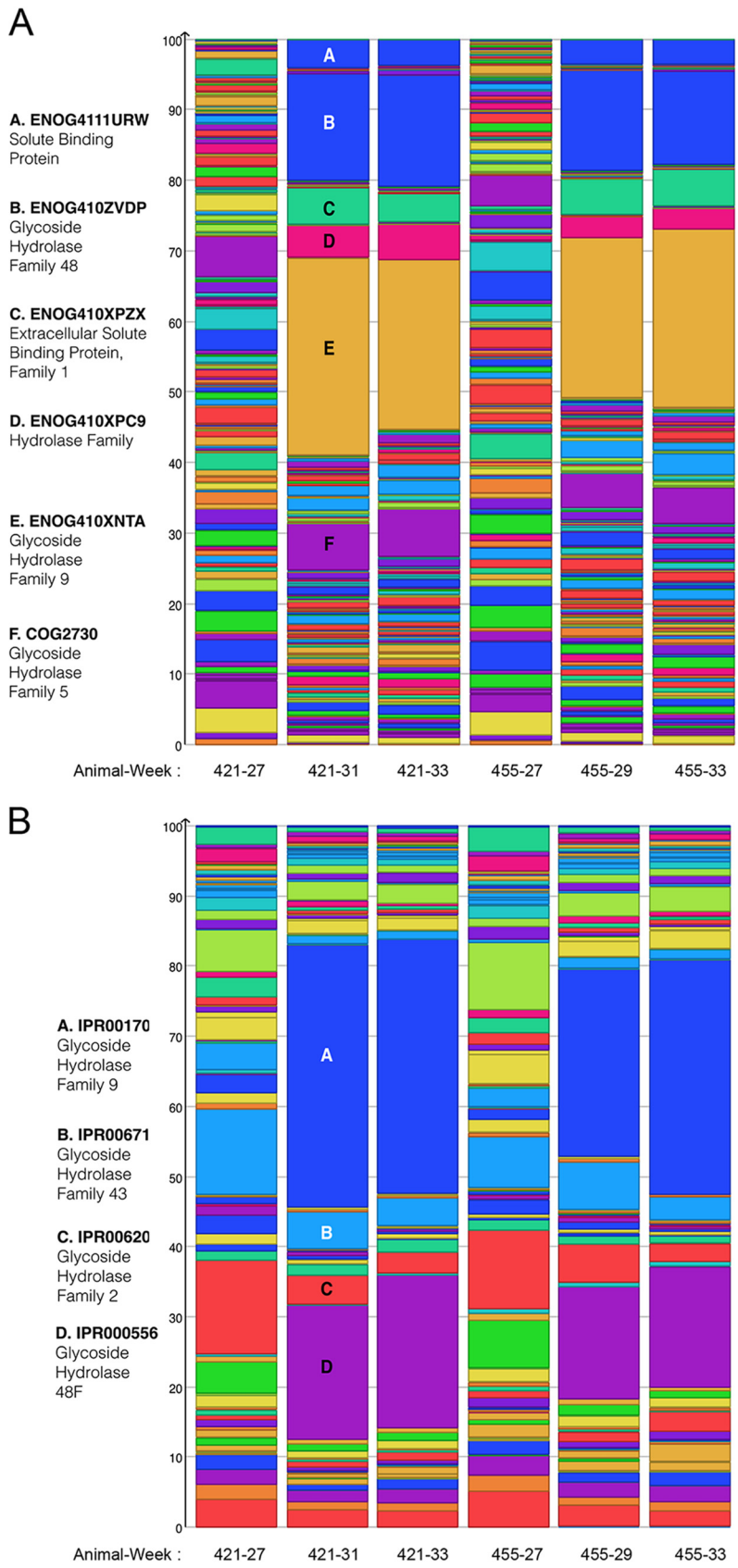


FIG 5 Expression profiles for eggnog/COG (clusters of orthologous groups) (A) and Interpro2GO categories (B). Counts were derived from functional assignments to the full metatranscriptome read data.

(Continued on next page)

Downloaded from https://journals.asm.org/journal/mbio on 08 September 2022 by 153.90.170.56.

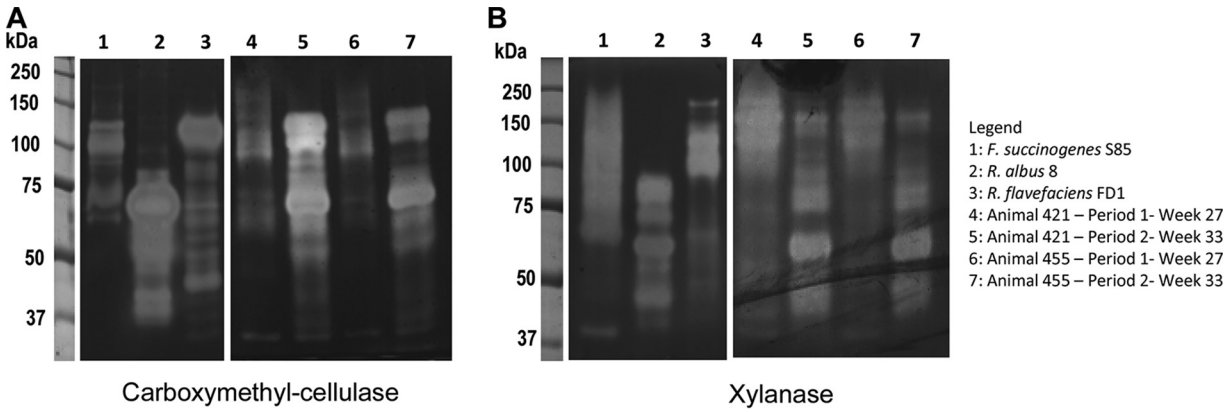


FIG 6 Zymogram profiles of carboxymethycellulases (A) and xylanases (B). Zymograms showing active enzyme profiles of pure cultures and present in protein extracts from the sheep rumen contents at the end of period 1 at week 27 (lane 4, animal 421; lane 6, animal 455) and of period 2 at week 33 (lane 5, animal 421; lane 7, animal 455). Zymogram profiles of protein extracts from *F. succinogenes* S85 (lane 1), *R. albus* 8 (lane 2), and *R. flavefaciens* (lane 3) after 48-h *in vitro* incubation on filter paper strips are presented for comparison.

Despite the obvious ecological advantages of *R. albus* and the competitiveness of *R. flavefaciens* both *in vitro* and in our model, with the exception of two studies (26, 27), most studies performed with conventional sheep have instead found *F. succinogenes* to outnumber both *Ruminococcus* spp. (28–32). The difference between *in vitro* studies, our animal model, and these studies on conventional sheep may be attributable to differences in the broader ecology, where a newborn immature microbiota could be more ecologically favorable to the development of *R. albus* and *R. flavefaciens*, while a conventional adult microbiota may better favor *F. succinogenes* through unmeasured ecological interactions. This assumption agrees with studies of newborn calves and lambs in which cellulolytic ruminococci colonized the rumen earlier than *F. succinogenes* (33, 34). Diet may also influence the composition of both the cellulolytic and broader community (32, 35–37).

F. succinogenes expressed a more diverse CAZyme repertoire that included GH8, GH51, GH5, and GH9 family glycoside hydrolases. These genes are also highly expressed in *in vitro* continuous cultures of *F. succinogenes* S85 (38) and include a functionally characterized GH51 endoglucanase 2 (Eg2, CelF, and EgF) and the GH9 endoglucanase 1 (Cel2 and End1). Our results suggest that GH8 CAZymes may also be important to the fibrolytic function of *F. succinogenes* on lucerne. Additionally, four *F. succinogenes* genes (FSU_2078, FSU_2396, FSU_2397, and FSU_2502) have previously been proposed from *in vitro* proteomics studies to encode a four-protein complex within outer membrane vesicles (8). These vesicles are hypothesized to serve as vehicles of CAZymes that target plant biomass by means of the 180-kDa cellulose-binding protein encoded by 1 of 10 Fibro-slime-domain-containing gene, FSU_2502. Our metatranscriptomic data confirmed the high expression of these four genes *in vivo* and also suggest that OMV formation may involve additional genes, including a cluster of eight highly expressed genes (FSU_RS11370 = FSU_2396 to FSU_RS11405 = FSU_2404). As transcriptional changes do not necessarily reflect the translation and activity of the associated enzymes, we accompanied the metatranscriptomic analyses with functional analyses using *in sacco* incubations, zymograms, and metabolomics.

DM disappearance varied over time, corresponding to differences in the relative

FIG 5 Legend (Continued)
(A) Overall counts for assignments to functions related to carbohydrate transport and metabolism (family G) were then determined using MEGAN, scaling to the overall percentage of each specific functional category, with the top six eggnog categories described. (B) Overall counts for assignments to functions related to carbohydrate metabolism (GO:0005975, carbohydrate metabolic process) were then determined using MEGAN, scaling to the overall percentage of each specific functional category, with the top four InterPro assignments shown.

Downloaded from https://journals.asm.org/journal/mbio on 08 September 2022 by 153.90.170.56.

TABLE 1 Fibrolytic enzyme specific activity in the sheep rumen contents pre- and postinoculation of *R. albus* and *R. flavefaciens*[a]

Enzyme	Enzyme sp act (mmol reducing sugars · mg protein^{-1} min^{-1})	
	Period 1, wk 27	Period 2, wk 33
CMCase	109 ± 46 A	278 ± 85 B
Xylanase	439 ± 127 A	1,140 ± 166 B

[a]Enzyme specific activity was measured from protein extracts prepared from the sheep rumen contents at the end of each period. Values are the means ± standard deviations (SD) of the data obtained for the two sheep and for rumen contents sampled pre- and postfeeding. Different letters after the values indicate significant difference at $P < 0.01$.

abundances of each cellulolytic species, but also between animals and by substrate and did not reflect measured CMCase and xylanase activities, which were 2.6-fold higher when ruminococci became dominant. This finding suggests that factors in addition to total fibrolytic enzyme activities must influence fibrolytic efficiency.

The resulting changes in fermentation end products, including a reduction in propionate and increases in acetate and butyrate, as the two *Ruminococcus* strains outcompeting *F. succinogenes* may impact the resulting productivity of the animal. Indeed, the amounts and profiles of short-chain fatty acids (SCFAs) formed in the rumen have consequences for the efficiency of energy utilization, production of methane, risks of ruminal acidosis, and composition of animal products (39, 40). *F. succinogenes* is an acetate and succinate producer, and succinate is a precursor of propionate (41). Our metatranscriptome data confirmed that two genes (FSU_RS14505 and FSU_RS14510) encoding fumarate reductase/succinate dehydrogenase involved in the succinate pathway were highly transcribed by *F. succinogenes in vivo*, which was not observed with the two ruminococci (data not shown). Hence, the disappearance of this species could in part explain the decrease in propionate. *R. albus* and *R. flavefaciens* produce acetate, formate, and hydrogen. All three products could account for the increase in acetate in rumen fluids knowing that formate and H_2 can be utilized by acetogenic bacteria to produce acetate. We previously showed that acetogenic bacteria were active in similar animal models as long as methanogens did not colonize the ecosystem at high levels (14). The increase in butyrate may indicate unmeasured ecological interactions that favor growth of butyrate-producing bacteria as ruminococci become dominant.

TABLE 2 Fiber degradation in the sheep rumen contents pre- and postinoculation of *R. albus* and *R. flavefaciens*[a]

Sheep and degradation process	Amt of lucerne (% (w/w) dry matter initial feed)		Amt of wheat straw cell walls (% (w/w) dry matter initial feed)	
	wk 23	wk 30	wk 25	wk 32
Sheep 421				
DMdis	20 ± 5 A	26 ± 2 B	19 ± 4 X	20 ± 2 X
NDFdis	12.5 ± 0.7 A	16.8 ± 0.2 B	18.1 ± 0.4	18.7 ± 0.2
ADFdis	9.2 ± 0.7 A	11.8 ± 0.2 B	10.9 ± 0.3	11.5 ± 0.4
Sheep 455				
DMdis	28 ± 1 A	26 ± 1 A	18 ± 2 X	7 ± 3 Y
NDFdis	17.5 ± 0.1 A	16.0 ± 0.2 B	19.2 ± 0.4 A	8.2 ± 1.1 B
ADFdis	13.7 ± 0.1 A	11.7 ± 0.1 B	11.2 ± 0.3 A	5.5 ± 0.2 B

[a]DMdis was measured from series of bags containing plant materials and incubated in the rumen for 24 h during either weeks 23 and 25 of period 1 or weeks 30 and 32 of period 2. The data obtained from the two animals were not averaged because at week 30 and week 32, the abundances of the three cellulolytic species had not evolved in the same manner in the two sheep as evidenced in Fig. 2. DMdis values are the means ± SD of the data obtained for each animal and each plant material. Different letters after the values indicate significant difference at $P < 0.005$. NDFdis and ADFdis values are the means of three fiber analysis determinations performed on pooled fermented residues retrieved from each bag series.

Downloaded from https://journals.asm.org/journal/mbio on 08 September 2022 by 153.90.170.56.

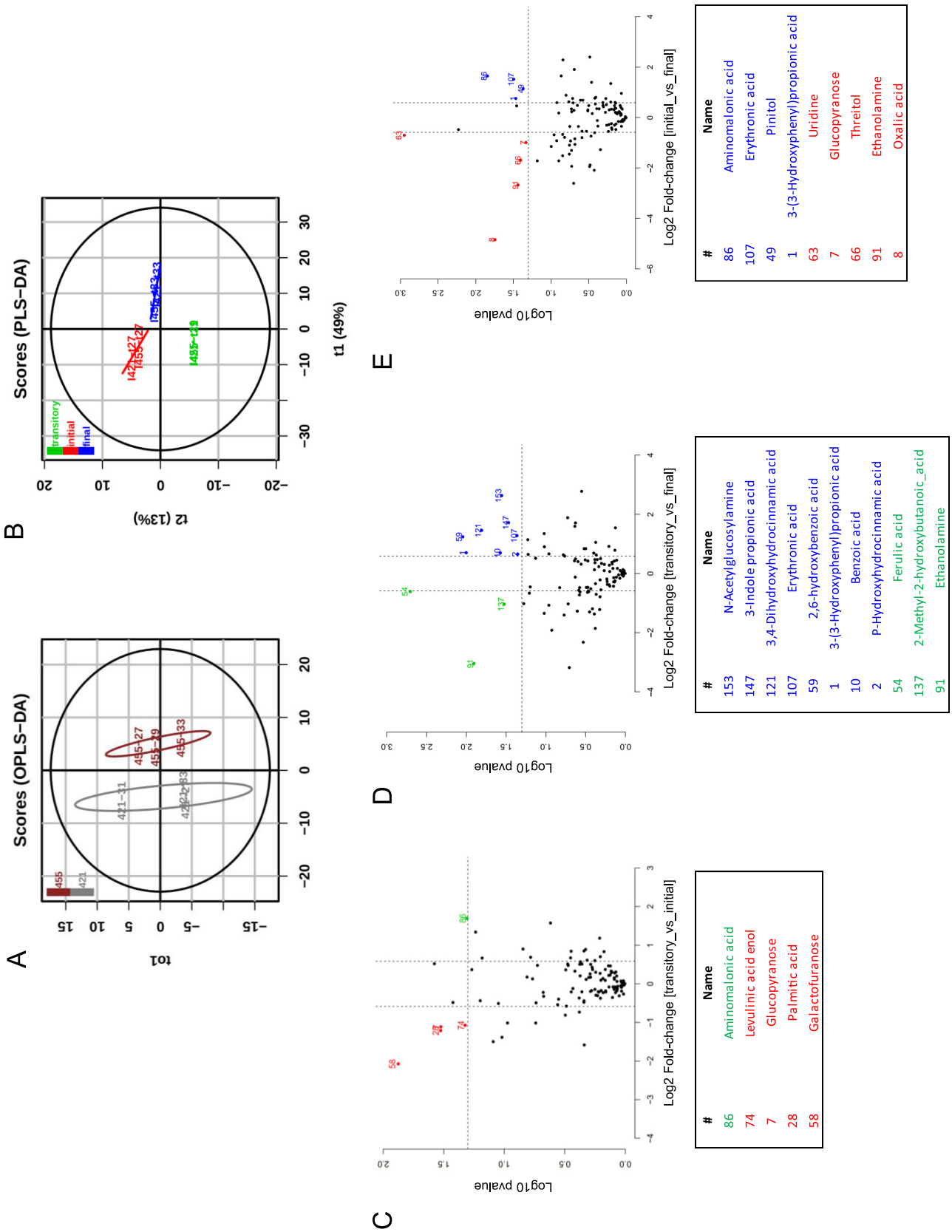


FIG 7 Metabolomic profiles according to animal (421 and 455) and sampling time. Sampling time was referred to as initial in red (week 27 for both animals), transitory in green (weeks 31 for 421 and week 29 for 455), and final in blue (week 33 for both animals). Variations in metabolomes were

(Continued on next page)

Downloaded from https://journals.asm.org/journal/mbio on 08 September 2022 by 153.90.170.56.

In addition to SCFAs, several phenolic metabolites, including 3-(3-hydroxyphenyl) propionic acid were found to change in association with the abundance of the two ruminococci. These metabolites are catabolites of plant polyphenols, including hydroxycinnamic acids (42). It is possible that the ruminococci enhance the production of these molecules by hydrolyzing esterified hydroxycinnamic acids from lucerne hemicelluloses. While phenolic metabolites exhibit antimicrobial properties, *R. albus* and *R. flavefaciens* may be resistant to these effects, given findings that the dehydroxylated derivative of 3-(3-hydroxyphenyl)propionic acid, 3-phenylpropanoic acid has instead been shown to enhance their growth and fibrolysis *in vitro* (43–46).

In conclusion, this study describes for the first time *in vivo* competition between the three predominant cellulolytic rumen bacteria. It shows that global metabolic modifications in the rumen can be engendered by a simple disequilibrium in the cellulolytic community. It also provides *in vivo* evidence of the expression by the three cellulolytic bacterial species of different enzymatic and structural systems previously thoroughly studied *in vitro* that allow them to ensure their adhesion and hydrolytic function and survive in a very complex and competitive microbial digestive ecosystem.

MATERIALS AND METHODS

Ethics statement. The experimental protocol was validated by the local ethics committee (Comité d'Ethique pour l'Experimentation Animale Auvergne) before beginning the trial, and the protocol was registered under the number CE18-08. Procedures were in accordance with the guidelines for animal research of the French Ministry of Agriculture and all other applicable national and European guidelines and regulations for experimentation with animals.

Animal model. The gnotobiotic sheep model has been described previously in detail (14, 47). Briefly, two INRAE line 401 lambs were born naturally and removed from their dams 17 h after birth. Lamb 421 (female) and lamb 455 (male) were then placed in a sterile isolator and reared under gnotobiotic conditions in the animal experimental facility of UMR MEDIS (Theix, Saint-Genes-Champanelle, France). Lambs were fed ultrahigh-temperature (UHT)-sterilized cow (*Bos taurus*) milk until they were 14 weeks old. At 2 weeks, they were also provided access to pelleted rations created from dehydrated lucerne (alfalfa) hay (7-mm diameter; SAFE, Augy, France). Lucerne pellets were sterilized by gamma irradiation (4 Mrad; Ionisos, Dagneux, France) prior to feeding. After 14 weeks, the animals were fed once daily at 8:00 a.m. with the lucerne pellets only. Sheep 421 and 455 were fitted within the sterile isolator with a permanent rumen plastisol cannula (diameter, 2.5 cm) at 17 and 18 weeks, respectively. Withdrawal of rumen contents and *in sacco* incubations began after the lambs had recovered from surgery at 22 weeks of age. The experiment ran for 12 weeks, and at the end of the experiment, sheep 421 and sheep 455 were both 34 weeks old and weighed 32 and 42 kg, respectively.

Cellulolytic inoculation. Lambs were monitored for the first 2 weeks after birth for the cultivable presence of cellulolytic and methanogenic activities, as well as for cultivable protozoa and fungi as previously described (14). None of these metabolisms or microbial groups were detected during this period. At 3 weeks of age, lambs were inoculated on 3 consecutive days with 20 ml (10^9 cells ml^{-1}) of a 2-day-old pure culture of *Fibrobacter succinogenes* S85 (ATCC 19169) fed on filter paper strips. The lambs were subsequently inoculated at 7 weeks of age with a pure culture of the ruminal methanogen *Methanobrevibacter* sp. 87.7 to enable hydrogenotrophy and ensure fibrolytic activity would not be inhibited by hydrogen buildup in this animal model (14, 47, 48). Finally, at 28 weeks of age, they were inoculated via cannula on 3 consecutive days with 160 ml (10^8 cells ml^{-1}) of 2-day-old pure cultures of both *Ruminococcus flavefaciens* FD1 (sourced from the Department of Animal Science, University of Illinois, Champaign-Urbana, IL, USA) and *Ruminococcus albus* 8 (sourced from USDA-National Center for Agricultural Utilization Research [NCAUR], Peoria, IL, USA) each supplied on filter paper strips. An overview of the animal trial and sampling procedure is presented in Fig. 1.

Rumen sampling. Rumen contents were withdrawn through the cannula on 2 consecutive days (each Tuesday and Wednesday) of weeks 22, 24, and 27 (*F. succinogenes* S85 was the only cellulolytic strain inoculated at these sample points) and on weeks 29, 31 and 33 (after *R. albus* 8 and *R. flavefaciens* FD1 had been inoculated) (Fig. 1). Sampling was performed before morning feeding (time zero [T0]) and 3 h after feeding (T3). T0 samples are reported with comparisons to T3 samples described in Text S1 in the supplemental material. The rumen content (50 ml) withdrawn on the first day of sampling was immediately used to determine ruminal pH and for culture-based microbial enumerations.

The rumen content (250 ml) withdrawn on the second day of sampling was treated as follows: a 50-

FIG 7 Legend (Continued)
visualized by OPLS-DA model score plot for the animal response (A) and by PLS-DA score plot for the time response (B). Discriminant metabolites are presented in volcano plots showing pairwise comparisons between initial versus transitory (C), transitory versus final (D), and initial versus final (E) sampling times. The dashed lines mark the significance thresholds adjusted to a *P* value of <0.05 and to a $\log_2$ fold change of >0.6 or less than -0.6 corresponding to a fold change of >1.5 or less than -1.5. Significant metabolites obtained for each comparison were colored according to sampling time and were given a number for the corresponding metabolite presented in the table below each plot. In the tables, a positive or negative $\log_2$ fold change means a higher abundance or lower abundance, respectively, at the sampling time defined by its color. Only the metabolites (= variable) with a variable importance projection (VIP) of >1.0 in the PLS-DA analysis were considered relevant for time discrimination.

Downloaded from https://journals.asm.org/journal/mbio on 08 September 2022 by 153.90.170.56.

ml aliquot was immediately mixed on ice with 100 ml RNAlater (Applied Biosystems, Courtaboeuf, France), aliquoted to four fractions of equal volumes, and stored at −80°C until nucleic acid extraction. A second 50-ml aliquot was kept on ice and treated as described below for polysaccharidase enzymatic analyses. A third 50-ml aliquot was frozen at −20°C (as sample saving) to determine the dry matter content of the rumen material. The remaining aliquot was centrifuged at 10,000 × *g* for 15 min at 4°C, and 1 ml of supernatant was taken and stored at −80°C for metabolomic analyses.

Enumeration of microbial communities. Total cultivable bacteria, total cultivable cellulolytic bacteria, and total cultivable methanogens were enumerated by using the most probable number (MPN) method as described previously (14).

***In sacco* digestibility assays.** To evaluate plant substrate degradation in our model, we used the lucerne (alfalfa) pellets, as provided in the animal diet, and cell walls prepared as described previously (49) from ground and sieved (160 to 400 μm) wheat straw. Cell wall residues were prepared using an Soxhlet extractor by refluxing in 1:2 ethanol-toluene and then 95°C ethanol until the extracts became colorless (49). Nylon bags (R510 *in situ* bags [100 × 50 mm; porosity of 50 μm]; Ankom Technology, NY, USA) were filled with either 1 g dry matter (DM) of the lucerne pellets or 0.5 g DM of wheat straw cell walls. *In sacco* incubations of lucerne bags were carried out for both sheep beginning on weeks 23 (post-fibrobacter inoculation but pre-ruminococci inoculation) and 30 (post-ruminococci inoculation), while incubations of wheat cell wall bags began on weeks 25 (also post-fibrobacter inoculation but pre-ruminococci inoculation) and 32 (post-ruminococci inoculation; Fig. 1). During 8 consecutive days, two bags were introduced into the rumen before morning feeding and removed after 24 h of incubation. One bag was then immediately washed in RNase-free phosphate-buffered saline (PBS) until the buffer was clear. It was then placed in a sterile tube containing a mixture of 20 ml RNAlater (Applied Biosystems, Courtaboeuf, France) and 10 ml RNase-free water and frozen at −80°C for subsequent molecular analyses. The other bag was washed with tap water until the water was visibly clear and then frozen at −20°C for subsequent fiber composition analysis. Extra bags were also incubated to provide materials for electron microscopy observations of adhering bacteria, as described below.

Dry matter disappearance was determined by measuring changes in the weight of nylon bags between insertion and after removal and drying at 60°C for at least 72 h. Contents of the bags corresponding to the same plant substrate, same week of incubation, and same animal were pooled together for analyses. Residues were analyzed for neutral detergent fiber (NDF) and acid detergent fiber (ADF) contents using the Ankom fiber analyzer (Ankom Technology, NY, USA). Unincubated (control) bags were treated identically and used to calculate the base lines of DM, NDF, and ADF disappearances (DMdis, NDFdis, and ADFdis, respectively).

Enzyme activity assays and zymograms. Microbial enzymes from rumen contents were recovered as follows: a freshly collected rumen sample (50 ml) was centrifuged at 10,000 × *g* for 15 min at 4°C, and the pellet was washed several times with an anaerobic mineral solution (50) until supernatant was clear. The washed pellet containing rumen microbes and lucerne residues was then frozen at −80°C until analysis. Thawed pellets (1 g) from weeks 27 and 33 (end of each period) were mixed with 5 ml phosphate buffer (50 mM, pH 7) containing the Complete protease inhibitor cocktail (Roche, Boulogne-Billancourt, France). Cell lysis was performed by sonication (four pulses of 30 s at 20 KHz and 60 W, separated by 1-min pause on ice). The resulting mixture was then centrifuged at 8,000 × *g* for 30 min at 4°C, and the supernatant was assayed for polysaccharidase specific activity and zymogram analysis as previously described (21), using carboxymethyl cellulose (medium viscosity) and oatspelt xylan (Sigma-Aldrich, Saint-Quentin-Fallavier, France) as the substrates.

Electron microcopy. The lucerne and wheat straw cell walls from the *in sacco* incubations were fixed with 3% glutaraldehyde in PBS for 1h at 4°C. They were then treated and examined with a Philips SEM 505 scanning electron microscope as described previously (21).

Nucleic acid extraction. Rumen contents and *sacco* residues, both in suspension in RNAlater (Applied Biosystems, Courtaboeuf, France) were thawed on ice and centrifuged at 15,000 × *g* for 15 min at 4°C, and the resulting supernatant was discarded. Pellets from *sacco* residues corresponding to the same plant substrate, same week of incubation, and same animal were pooled to obtain sufficient quantities of material for nucleic acid extraction. DNA was extracted in triplicate from 0.25 g of pellet using an MP Biomedical DNA extraction and purification kit (Fast DNA Spin kit and Gene Clean Turbo; MP Biomedicals, Illkirch, France) following the manufacturer's recommendations. RNA was extracted in quadruplicate from 0.70 g of rumen content pellet using a Nucleospin RNAII kit (Macherey-Nagel, Hoerdt, France) following the supplier's instructions with the following exceptions. (i) During the cell lysis step, approximately 160-mg zirconia beads of 0.1-mm diameter (Bio Spec Products, Bartlesville, OK, USA) were added to the sample in addition to RA1 buffer and β-mercaptoethanol, for bead-beating (twice for 30 s each time at maximum power of 6.5) using the FastPrep instrument (MP Biomedicals, Illkirch, France). (ii) During the washing step, buffer RA2 was replaced by buffer FW1 as recommended by the supplier. Eluted RNA was submitted to an additional RNase-free DNase treatment (provided in the RNAII kit). RNA integrity was assessed using an Agilent 2100 bioanalyzer as previously described (51), and all samples were found to have a RNA integrity number (RIN) of >8. Nucleic acid concentrations were estimated by absorbance at 260 nm (NanoDrop ND-1000). They were kept at −80°C until utilization.

Quantitative real-time PCR. Quantitative PCR (qPCR) targeting total bacteria, methanogenic archaea, and each of the cellulolytic species—*R. albus*, *R. flavefaciens*, and *F. succinogenes*—was performed using SYBR green chemistry with a Mastercycler ep realplex 2S (Eppendorf, Le Pecq, France) in 96-well plates (Twin.tec plate 96 skirted; Eppendorf). Results were analyzed using realplex version 2.0 software (Eppendorf). The qPCR conditions (i.e., primers, reaction mixture, program, standard curves) have been

Downloaded from https://journals.asm.org/journal/mbio on 08 September 2022 by 153.90.170.56.

TABLE 3 Genomes used in this study

Strain	BioProject ID	NCBI accession no.
Fibrobacter succinogenes subsp. *succinogenes* S85	PRJNA224116	NC_017448.1
Methanobrevibacter sp. 87.7	PRJNA339853	MRCT00000000.1
Ruminococcus albus 8	PRJNA224116	NZ_ADKM00000000.2
Ruminococcus flavefaciens FD-1	PRJNA224116	NZ_ACOK01000031.1

described previously (29), except that we used the IQ SYBR Green Supermix (Bio-Rad, Marnes-la-Coquette, France). qPCRs were performed in triplicate from three separate extracts of DNA per sample (biological replicates). Results were expressed as *rrs* copies of microbial target per gram (dry matter) of sample (centrifuged rumen content or *sacco* residue).

Genomic reference data. Representative genomes from each of the cellulolytic species have previously been reported for *R. flavefaciens* 17 (52), *R. albus* 8 (53), and *Fibrobacter succinogenes* S85 (54). *Methanobrevibacter* sp. 87.7 was sequenced at Montana State University via a single run of an Illumina MiSeq. DNA was extracted using the DNeasy PowerLyzer microbial kit (Qiagen, Germantown, MD, USA), and genomic data were assembled using SPAdes v. 3.6.2 and gave 500-fold coverage. Genomic data were annotated using NCBI's Prokaryotic Genome Annotation Pipeline (https://www.ncbi.nlm.nih.gov/genome/annotation_prok/) and are deposited in GenBank under NZ_MRCT01000000 and BioProject PRJNA339853. The four genomes used as reference in this study are presented in Table 3.

Metagenomic and metatranscriptomic analyses. Rumen samples withdrawn before feeding (time zero [T0]) at weeks 27, 31, and 33 for animal 421 and weeks 27, 29, and 33 for animal 455 (Fig. 1) were subjected to metagenomic and metatranscriptomic analyses. Triplicate DNA and quadruple RNA extracts were each pooled by animal and time point. RNA extracts were transcribed to cDNA by first strand cDNA synthesis, and both DNA and cDNA were independently sequenced with one lane each of paired-end 2 × 125 nucleotide (nt) HiSeq 2500 (Illumina) sequencing.

Sequence data were quality and adapter trimmed using Trimmomatic v 0.33 (55). Metatranscriptome data were then further preprocessed using SortMeRNA v 2.1b (56) to separate sequences into rRNA and non-rRNA fractions. Full metagenomic data and the rRNA and non-rRNA subset of metatranscriptomic data from the SortMeRNA analysis were aligned to all four reference genomes as a single index file, using the Burrows-Wheeler Aligner v 0.7.15 (57). Coverage data for all alignments (used for downstream visualization) were generated using deepTools v. 2.5.0.1 (58) and visualized using the Integrative Genomics Viewer v2.3.92 (59). Basic expression normalization to reads per kilobase per million (RPKM) was performed using the edgeR v3.18.1 package in R v3.4.0 (60). Heat-maps were generated using the R package, ggplots on expression data scaled to the standard deviation from the mean. *De novo* CAZy-specific functional analysis was performed using HMMER v 3.1b2 (61) and the Release 5.0 protein motifs obtained from dbCAN (62). Read counts for all coding sequence annotation from each genome were generated using featureCounts v1.9.2 (63). All metagenomic and metatranscriptomic data were aligned using DIAMOND v. 0.8.37 (64) against the NCBI nonredundant protein database (July 2017). Taxonomic and functional information assignment as well as initial analyses and summary figures for taxonomic and functional classification were generated using MEGAN v6.8.13 (65). Metagenomic and metatranscriptomic data are deposited in GenBank under BioProject PRJNA646650.

Metabolomic analyses. Using complementary samples to those utilized for metagenomic and metatranscriptomic analyses, 1 ml of the rumen supernatant (collected as described above) was dried and derivatized as previously described (66). A 5-μl aliquot of an internal standard (C_{31} fatty acid) was added to each sample prior to derivatization. Samples were injected with a split ratio of 7:1 into a gas chromatography (GC)-mass spectrometry (MS) system, consisting of an Agilent 7890A (Agilent Inc., Palo Alto, CA, USA) gas chromatograph, an Agilent 5975C mass selective detector, and an Agilent 7683B autosampler. Gas chromatography was performed on 60-m HP-5MS columns with 0.25-mm inner diameter and 0.25-mm film thickness (Agilent Inc., Palo Alto, CA, USA) and with an injection temperature of 2,500°C, the interface set at 2,500°C, and the ion source adjusted to 2,300°C. The helium carrier gas was set at a constant flow rate of 1.5 ml min^{-1}. The temperature program of 5-min isothermal heating at 700°C, followed by an oven temperature increase of 50°C min^{-1} to 3,100°C and a final 20 min at 3,100°C. The mass spectrometer was operated in positive electron impact mode (EI) at 69.9 eV ionization energy in the *m/z* 30 to 800 scan range. The spectra of all chromatogram peaks were then compared with electron impact mass spectrum libraries NIST08 (National Institute of Standards and Technology [NIST], MD, USA) and WILEY08 (Palisade Corporation, NY, USA) and a custom library of the University of Illinois Roy J. Carver Metabolomics Center. To allow direct comparisons between samples, all data were normalized to the internal standard in each chromatogram. The chromatograms and mass spectra were evaluated using the MSD ChemStation (Agilent, Palo Alto, CA, USA) and AMDIS (NIST, Gaithersburg, MD, USA). The retention time and mass spectra were implemented within the AMDIS method formats.

Analysis of volatile fatty acid (VFA) was performed without derivatization on rumen fluids using gas chromatography as previously described (67). Fermentation end products were assessed by comparing prefeeding (0-h) and 3-h postfeeding profiles throughout the animal experiment.

Statistical analyses. A Student's *t* test was used to compare DM disappearance, as well as polysaccharidase specific activities in animals between period 1 (weeks 22 to 27) with *F. succinogenes* only and period 2 (weeks 28 to 33) after inoculation of cellulolytic ruminococci. Differences were considered significant at $P < 0.05$.

Downloaded from https://journals.asm.org/journal/mbio on 08 September 2022 by 153.90.170.56.

Metabolomic data were analyzed by using a partial least-squares discriminant analysis (PLS-DA) model to visualize variations of metabolites among experimental time points (initial [week 27], transitory [weeks 29 to 31], and final [week 33]) and an orthogonal PLS-DA for the two animals (421 and 455). The raw matrix with metabolite concentrations was $\log_{10}$ transformed before analyzing the data with the ropls R package (68, 69). To identify the metabolites responsible for discrimination between two time points (initial versus transitory, transitory versus final, and initial versus final), a pairwise comparative analysis using a *t* test was used to test the statistical significance. Only the variables (metabolites) with a variable importance projection (VIP) of >1.0 in the PLS-DA analysis were considered relevant for time discrimination. These tests were performed using the MetaboDiff R package (70) and were normalized using the variance stabilization method (71) before the differential analyses.

Data availability. The data sets supporting the results of this article are included within the article and its additional supplemental material. The genome sequence of *Methanobrevibacter* sp. 87.7 was deposited in GenBank under NZ_MRCT01000000 and BioProject PRJNA339853. The metagenome and metatranscriptome data are available in GEO data sets at NCBI (http://www.ncbi.nlm.nih.gov/) under BioProject PRJNA646650.

SUPPLEMENTAL MATERIAL

Supplemental material is available online only.

TEXT S1, DOCX file, 0.04 MB.

FIG S1, PDF file, 0.1 MB.

FIG S2, PDF file, 0.1 MB.

FIG S3, PDF file, 0.1 MB.

FIG S4, PDF file, 0.4 MB.

FIG S5, PDF file, 0.1 MB.

FIG S6, PDF file, 0.2 MB.

FIG S7, PDF file, 0.2 MB.

TABLE S1, XLSX file, 0.3 MB.

TABLE S2, XLSX file, 0.03 MB.

ACKNOWLEDGMENTS

We thank Christel Bera-Maillet for advice regarding the experimental protocol for obtaining gnotobiotically raised sheep and B. Gaillard-Martinie who was in charge of the electron microscopy work. We also thank Gérard Andant and Gérard Vert for technical assistance, especially for their input in the maintenance, sampling, and analyses performed on these animals maintained for several months in sterile isolators.

This work was funded by MEDIS laboratory (INRAE France) with support from the Roy J. Carver Biotechnology Center, the Montana Agricultural Experiment Station (project MONB00113), the National Institute of General Medical Sciences of the National Institutes of Health (NIH-NIGMS; award number P20GM103474) and is a contributing project to Multistate Research Projects, W4177, Enhancing the Competitiveness of U.S. Beef (MONB00195).

We declare that we have no competing interests.

P.M. and B.A.W. conceived the study. C.J.Y., P.L., and P.M. performed the experiments. C. J.Y., C.J.F., P.R., E.F., and P.M. analyzed the data. C.J.Y. and P.M. wrote the manuscript with the help of all authors. All authors read and approved the final manuscript.

REFERENCES

1. Pauly M, Keegstra K. 2008. Cell-wall carbohydrates and their modification as a resource for biofuels. Plant J 54:559–568. https://doi.org/10.1111/j.1365-313X.2008.03463.x.
2. Yeoman CJ, White BA. 2014. Gastrointestinal tract microbiota and probiotics in production animals. Annu Rev Anim Biosci 2:469–486. https://doi.org/10.1146/annurev-animal-022513-114149.
3. Henderson G, Cox F, Ganesh S, Jonker A, Young W, Global Rumen Census Collaborators, Janssen PH. 2015. Rumen microbial community composition varies with diet and host, but a core microbiome is found across a wide geographical range. Sci Rep 5:14567. https://doi.org/10.1038/srep14567.
4. Kong YH, Xia Y, Seviour R, He ML, McAllister T, Forster R. 2012. In situ identification of carboxymethyl cellulose-digesting bacteria in the rumen of cattle fed alfalfa or triticale. FEMS Microbiol Ecol 80:159–167. https://doi.org/10.1111/j.1574-6941.2011.01295.x.
5. Morais S, Mizrahi I. 2019. Islands in the stream: from individual to communal fiber degradation in the rumen ecosystem. FEMS Microbiol Rev 43:362−379. https://doi.org/10.1093/femsre/fuz007.
6. Jindou S, Borovok I, Rincon MT, Flint HJ, Antonopoulos DA, Berg ME, White BA, Bayer EA, Lamed R. 2006. Conservation and divergence in cellulosome architecture between two strains of *Ruminococcus flavefaciens*. J Bacteriol 188:7971–7976. https://doi.org/10.1128/JB.00973-06.
7. Dassa B, Borovok I, Ruimy-Israeli V, Lamed R, Flint HJ, Duncan SH, Henrissat B, Coutinho P, Morrison M, Mosoni P, Yeoman CJ, White BA, Bayer EA. 2014. Rumen cellulosomics: divergent fiber-degrading strategies revealed by comparative genome-wide analysis of six ruminococcal strains. PLoS One 9: e99221. https://doi.org/10.1371/journal.pone.0099221.
8. Arntzen MO, Varnai A, Mackie RI, Eijsink VGH, Pope PB. 2017. Outer membrane vesicles from *Fibrobacter succinogenes* S85 contain an array of

Downloaded from https://journals.asm.org/journal/mbio on 08 September 2022 by 153.90.170.56.

carbohydrate-active enzymes with versatile polysaccharide-degrading capacity. Environ Microbiol 19:2701–2714. https://doi.org/10.1111/1462-2920.13770.
9. Raut MP, Couto N, Karunakaran E, Biggs CA, Wright PC. 2019. Deciphering the unique cellulose degradation mechanism of the ruminal bacterium *Fibrobacter succinogenes* S85. Sci Rep 9:16542. https://doi.org/10.1038/s41598-019-52675-8.
10. Mosoni P, Fonty G, Gouet P. 1997. Competition between ruminal cellulolytic bacteria for adhesion to cellulose. Curr Microbiol 35:44–47. https://doi.org/10.1007/s002849900209.
11. Shi Y, Weimer PJ. 1997. Competition for cellobiose among three predominant ruminal cellulolytic bacteria under substrate-excess and substrate-limited conditions. Appl Environ Microbiol 63:743–748. https://doi.org/10.1128/AEM.63.2.743-748.1997.
12. Chen J, Weimer P. 2001. Competition among three predominant ruminal cellulolytic bacteria in the absence or presence of non-cellulolytic bacteria. Microbiology (Reading) 147:21–30. https://doi.org/10.1099/00221287-147-1-21.
13. Chaucheyras-Durand F, Masseglia S, Fonty G, Forano E. 2010. Influence of the composition of the cellulolytic flora on the development of hydrogenotrophic microorganisms, hydrogen utilization, and methane production in the rumens of gnotobiotically reared lambs. Appl Environ Microbiol 76:7931–7937. https://doi.org/10.1128/AEM.01784-10.
14. Gagen EJ, Mosoni P, Denman SE, Al Jassim R, McSweeney CS, Forano E. 2012. Methanogen colonisation does not significantly alter acetogen diversity in lambs isolated 17 h after birth and raised aseptically. Microb Ecol 64:628–640. https://doi.org/10.1007/s00248-012-0024-z.
15. Odenyo AA, Mackie RI, Stahl DA, White BA. 1994. The use of 16S rRNA-targeted oligonucleotide probes to study competition between ruminal fibrolytic bacteria: pure-culture studies with cellulose and alkaline peroxide-treated wheat straw. Appl Environ Microbiol 60:3697–3703. https://doi.org/10.1128/AEM.60.10.3697-3703.1994.
16. Pegden RS, Larson MA, Grant RJ, Morrison M. 1998. Adherence of the Gram-positive bacterium *Ruminococcus albus* to cellulose and identification of a novel form of cellulose-binding protein which belongs to the Pil family of proteins. J Bacteriol 180:5921–5927. https://doi.org/10.1128/JB.180.22.5921-5927.1998.
17. Rakotoarivonina H, Jubelin G, Hebraud M, Gaillard-Martinie B, Forano E, Mosoni P. 2002. Adhesion to cellulose of the Gram-positive bacterium *Ruminococcus albus* involves type IV pili. Microbiology (Reading) 148:1871–1880. https://doi.org/10.1099/00221287-148-6-1871.
18. Rakotoarivonina H, Larson MA, Morrison M, Girardeau JP, Gaillard-Martinie B, Forano E, Mosoni P. 2005. The *Ruminococcus albus pilA1-pilA2* locus: expression and putative role of two adjacent *pil* genes in pilus formation and bacterial adhesion to cellulose. Microbiology (Reading) 151:1291–1299. https://doi.org/10.1099/mic.0.27735-0.
19. Devillard E, Goodheart DB, Karnati SK, Bayer EA, Lamed R, Miron J, Nelson KE, Morrison M. 2004. *Ruminococcus albus* 8 mutants defective in cellulose degradation are deficient in two processive endocellulases, Cel48A and Cel9B, both of which possess a novel modular architecture. J Bacteriol 186:136–145. https://doi.org/10.1128/jb.186.1.136-145.2004.
20. Rakotoarivonina H, Terrie C, Chambon C, Forano E, Mosoni P. 2009. Proteomic identification of CBM37-containing cellulases produced by the rumen cellulolytic bacterium *Ruminococcus albus* 20 and their putative involvement in bacterial adhesion to cellulose. Arch Microbiol 191:379–388. https://doi.org/10.1007/s00203-009-0463-1.
21. Mosoni P, Gaillard-Martinie B. 2001. Characterization of a spontaneous adhesion-defective mutant of *Ruminococcus albus* strain 20. Arch Microbiol 176:52–61. https://doi.org/10.1007/s002030100292.
22. Vodovnik M, Duncan SH, Reid MD, Cantlay L, Turner K, Parkhill J, Lamed R, Yeoman CJ, Miller MEB, White BA, Bayer EA, Marinsek-Logar R, Flint HJ. 2013. Expression of cellulosome components and type IV pili within the extracellular proteome of *Ruminococcus flavefaciens* 007. PLoS One 8:e65333. https://doi.org/10.1371/journal.pone.0065333.
23. Odenyo AA, Mackie RI, Stahl DA, White BA. 1994. The use of 16S rRNA-targeted oligonucleotide probes to study competition between ruminal fibrolytic bacteria: development of probes for Ruminococcus species and evidence for bacteriocin production. Appl Environ Microbiol 60:3688–3696. https://doi.org/10.1128/AEM.60.10.3688-3696.1994.
24. Chen JQ, Stevenson DM, Weimer PJ. 2004. Albusin B, a bacteriocin from the ruminal bacterium Ruminococcus albus 7 that inhibits growth of Ruminococcus flavefaciens. Appl Environ Microbiol 70:3167–3170. https://doi.org/10.1128/aem.70.5.3167-3170.2004.
25. Azevedo AC, Bento CBP, Ruiz JC, Queiroz MV, Mantovani HC. 2015. Distribution and genetic diversity of bacteriocin gene clusters in rumen microbial genomes. Appl Environ Microbiol 81:7290–7304. https://doi.org/10.1128/AEM.01223-15.
26. Mosoni P, Chaucheyras-Durand F, Bera-Maillet C, Forano E. 2007. Quantification by real-time PCR of cellulolytic bacteria in the rumen of sheep after supplementation of a forage diet with readily fermentable carbohydrates: effect of a yeast additive. J Appl Microbiol 103:2676–2685. https://doi.org/10.1111/j.1365-2672.2007.03517.x.
27. Bekele AZ, Koike S, Kobayashi Y. 2010. Genetic diversity and diet specificity of ruminal *Prevotella* revealed by 16S rRNA gene-based analysis. FEMS Microbiol Lett 305:49–57. https://doi.org/10.1111/j.1574-6968.2010.01911.x.
28. Kobayashi Y, Shinkai T, Koike S. 2008. Ecological and physiological characterization shows that *Fibrobacter succinogenes* is important in rumen fiber digestion – review. Folia Microbiol (Praha) 53:195–200. https://doi.org/10.1007/s12223-008-0024-z.
29. Mosoni P, Martin C, Forano E, Morgavi DP. 2011. Long-term defaunation increases the abundance of cellulolytic ruminococci and methanogens but does not affect the bacterial and methanogen diversity in the rumen of sheep. J Anim Sci 89:783–791. https://doi.org/10.2527/jas.2010-2947.
30. Ghasemi S, Naserian AA, Valizadeh R, Vakili AR, Behgar M, Tahmasebi AM, Ghovvati S. 2012. Partial and total substitution of alfalfa hay by pistachio byproduct modulated the counts of selected cellulolytic ruminal bacteria attached to alfalfa hay in sheep. Livest Sci 150:342–348. https://doi.org/10.1016/j.livsci.2012.09.024.
31. Lettat A, Noziere P, Silberberg M, Morgavi DP, Berger C, Martin C. 2012. Rumen microbial and fermentation characteristics are affected differently by bacterial probiotic supplementation during induced lactic and subacute acidosis in sheep. BMC Microbiol 12:142. https://doi.org/10.1186/1471-2180-12-142.
32. Saro C, Ranilla MJ, Carro MD. 2012. Postprandial changes of fiber-degrading microbes in the rumen of sheep fed diets varying in type of forage as monitored by real-time PCR and automated ribosomal intergenic spacer analysis. J Anim Sci 90:4487–4494. https://doi.org/10.2527/jas.2012-5265.
33. Jami E, Israel A, Kotser A, Mizrahi I. 2013. Exploring the bovine rumen bacterial community from birth to adulthood. ISME J 7:1069–1079. https://doi.org/10.1038/ismej.2013.2.
34. Chaucheyras-Durand F, Ameilbonne A, Auffret P, Bernard M, Mialon MM, Duniere L, Forano E. 2019. Supplementation of live yeast based feed additive in early life promotes rumen microbial colonization and fibrolytic potential in lambs. Sci Rep 9:19216. https://doi.org/10.1038/s41598-019-55825-0.
35. Tajima K, Aminov RI, Nagamine T, Matsui H, Nakamura M, Benno Y. 2001. Diet-dependent shifts in the bacterial population of the rumen revealed with real-time PCR. Appl Environ Microbiol 67:2766–2774. https://doi.org/10.1128/AEM.67.6.2766-2774.2001.
36. Zhang J, Shi HT, Wang YJ, Li SL, Cao ZJ, Ji SK, He Y, Zhang HT. 2017. Effect of dietary forage to concentrate ratios on dynamic profile changes and interactions of ruminal microbiota and metabolites in Holstein heifers. Front Microbiol 8:2206. https://doi.org/10.3389/fmicb.2017.02206.
37. Wang LJ, Zhang GN, Xu HJ, Xin HS, Zhang YG. 2019. Metagenomic analyses of microbial and carbohydrate-active enzymes in the rumen of Holstein cows fed different forage-to-concentrate ratios. Front Microbiol 10:649. https://doi.org/10.3389/fmicb.2019.00649.
38. Neumann AP, Weimer PJ, Suen G. 2018. A global analysis of gene expression in Fibrobacter succinogenes S85 grown on cellulose and soluble sugars at different growth rates. Biotechnol Biofuels 11:295. https://doi.org/10.1186/s13068-018-1290-x.
39. Bergman EN. 1990. Energy contributions of volatile fatty-acids from the gastrointestinal-tract in various species. Physiol Rev 70:567–590. https://doi.org/10.1152/physrev.1990.70.2.567.
40. Noziere P, Glasser F, Sauvant D. 2011. In vivo production and molar percentages of volatile fatty acids in the rumen: a quantitative review by an empirical approach. Animal 5:403–414. https://doi.org/10.1017/S1751731110002016.
41. Louis P, Flint HJ. 2017. Formation of propionate and butyrate by the human colonic microbiota. Environ Microbiol 19:29–41. https://doi.org/10.1111/1462-2920.13589.
42. Stalmach A, Edwards CA, Wightman JD, Crozier A. 2013. Colonic catabolism of dietary phenolic and polyphenolic compounds from Concord grape juice. Food Funct 4:52–62. https://doi.org/10.1039/c2fo30151b.
43. Odenyo AA, Mackie RI, Fahey GC, Jr, White BA. 1991. Degradation of wheat straw and alkaline hydrogen peroxide-treated wheat straw by Ruminococcus albus 8 and Ruminococcus flavefaciens FD-1. J Anim Sci 69:819–826. https://doi.org/10.2527/1991.692819x.

Downloaded from https://journals.asm.org/journal/mbio on 08 September 2022 by 153.90.170.56.

44. Morrison M, Mackie RI, Kistner A. 1990. 3-Phenylpropanoic acid improves the affinity of Ruminococcus albus for cellulose in continuous culture. Appl Environ Microbiol 56:3220–3222. https://doi.org/10.1128/AEM.56.10.3220-3222.1990.
45. Stack RJ, Cotta MA. 1986. Effect of 3-phenylpropanoic acid on growth of and cellulose utilization by cellulolytic ruminal bacteria. Appl Environ Microbiol 52:209–210. https://doi.org/10.1128/AEM.52.1.209-210.1986.
46. Reveneau C, Adams SE, Cotta MA, Morrison M. 2003. Phenylacetic and phenylpropionic acids do not affect xylan degradation by *Ruminococcus albus*. Appl Environ Microbiol 69:6954–6958. https://doi.org/10.1128/aem.69.11.6954-6958.2003.
47. Chaucheyras-Durand F, Fonty G. 2001. Establishment of cellulolytic bacteria and development of fermentative activities in the rumen of gnotobiotically-reared lambs receiving the microbial additive *Saccharomyces cerevisiae* Cncm I-1077. Reprod Nutr Dev 41:57–68. https://doi.org/10.1051/rnd:2001112.
48. Piao H, Lachman M, Malfatti S, Sczyrba A, Knierim B, Auer M, Tringe SG, Mackie RI, Yeoman CJ, Hess M. 2014. Temporal dynamics of fibrolytic and methanogenic rumen microorganisms during in situ incubation of switchgrass determined by 16S rRNA gene profiling. Front Microbiol 5:307. https://doi.org/10.3389/fmicb.2014.00307.
49. Mosoni P, Besle JM, Cornu A, Duran H, Jouany JP. 1993. Wheat lignin labeling using [(U-C)-C-14] phenylanaline or [(O-CH3)-C-14)] sinapic acid for fermentation studies. J Agric Food Chem 41:1349–1354. https://doi.org/10.1021/jf00033a001.
50. Bryant MP, Burkey LA. 1953. Numbers and some predominant groups of bacteria in the rumen of cows fed different rations. J Dairy Sci 36:218–224. https://doi.org/10.3168/jds.S0022-0302(53)91483-0.
51. Bera-Maillet C, Mosoni P, Kwasiborski A, Suau F, Ribot Y, Forano E. 2009. Development of a RT-qPCR method for the quantification of *Fibrobacter succinogenes* S85 glycoside hydrolase transcripts in the rumen content of gnotobiotic and conventional sheep. J Microbiol Methods 77:8–16. https://doi.org/10.1016/j.mimet.2008.11.009.
52. Miller MEB, Yeoman CJ, Chia N, Tringe SG, Angly FE, Edwards RA, Flint HJ, Lamed R, Bayer EA, White BA. 2012. Phage-bacteria relationships and CRISPR elements revealed by a metagenomic survey of the rumen microbiome. Environ Microbiol 14:207–227. https://doi.org/10.1111/j.1462-2920.2011.02593.x.
53. Brulc JM, Yeoman CJ, Wilson MK, Miller MEB, Jeraldo P, Jindou S, Goldenfeld N, Flint HJ, Lamed R, Borovok I, Vodovnik M, Nelson KE, Bayer EA, White BA. 2011. Cellulosomics, a gene-centric approach to investigating the intraspecific diversity and adaptation of *Ruminococcus flavefaciens* within the rumen. PLoS One 6:e25329. https://doi.org/10.1371/journal.pone.0025329.
54. Suen G, Weimer PJ, Stevenson DM, Aylward FO, Boyum J, Deneke J, Drinkwater C, Ivanova NN, Mikhailova N, Chertkov O, Goodwin LA, Currie CR, Mead D, Brumm PJ. 2011. The complete genome sequence of *Fibrobacter succinogenes* S85 reveals a cellulolytic and metabolic specialist. PLoS One 6:e18814. https://doi.org/10.1371/journal.pone.0018814.
55. Bolger AM, Lohse M, Usadel B. 2014. Trimmomatic: a flexible trimmer for Illumina sequence data. Bioinformatics 30:2114–2120. https://doi.org/10.1093/bioinformatics/btu170.
56. Kopylova E, Noe L, Touzet H. 2012. SortMeRNA: fast and accurate filtering of ribosomal RNAs in metatranscriptomic data. Bioinformatics 28:3211–3217. https://doi.org/10.1093/bioinformatics/bts611.
57. Li H, Durbin R. 2009. Fast and accurate short read alignment with Burrows-Wheeler transform. Bioinformatics 25:1754–1760. https://doi.org/10.1093/bioinformatics/btp324.
58. Ramirez F, Dundar F, Diehl S, Gruning BA, Manke T. 2014. deepTools: a flexible platform for exploring deep-sequencing data. Nucleic Acids Res 42:W187–W191. https://doi.org/10.1093/nar/gku365.
59. Robinson JT, Thorvaldsdottir H, Winckler W, Guttman M, Lander ES, Getz G, Mesirov JP. 2011. Integrative genomics viewer. Nat Biotechnol 29:24–26. https://doi.org/10.1038/nbt.1754.
60. Robinson MD, McCarthy DJ, Smyth GK. 2010. edgeR: a Bioconductor package for differential expression analysis of digital gene expression data. Bioinformatics 26:139–140. https://doi.org/10.1093/bioinformatics/btp616.
61. Eddy SR. 1998. Profile hidden Markov models. Bioinformatics 14:755–763. https://doi.org/10.1093/bioinformatics/14.9.755.
62. Yin YB, Mao XZ, Yang JC, Chen X, Mao FL, Xu Y. 2012. dbCAN: a web resource for automated carbohydrate-active enzyme annotation. Nucleic Acids Res 40:W445–W451. https://doi.org/10.1093/nar/gks479.
63. Liao Y, Smyth GK, Shi W. 2014. FeatureCounts: an efficient general purpose program for assigning sequence reads to genomic features. Bioinformatics 30:923–930. https://doi.org/10.1093/bioinformatics/btt656.
64. Buchfink B, Xie C, Huson DH. 2015. Fast and sensitive protein alignment using DIAMOND. Nat Methods 12:59–60. https://doi.org/10.1038/nmeth.3176.
65. Huson DH, Auch AF, Qi J, Schuster SC. 2007. MEGAN analysis of metagenomic data. Genome Res 17:377–386. https://doi.org/10.1101/gr.5969107.
66. Roessner U, Wagner C, Kopka J, Trethewey RN, Willmitzer L. 2000. Technical advance: simultaneous analysis of metabolites in potato tuber by gas chromatography-mass spectrometry. Plant J 23:131–142. https://doi.org/10.1046/j.1365-313x.2000.00774.x.
67. Erwin ES, Marco GJ, Emery EM. 1961. Volatile fatty acid analyses of blood and rumen fluid by gas chromatography. J Dairy Sci 44:1768–1771. https://doi.org/10.3168/jds.S0022-0302(61)89956-6.
68. R Core Team. 2019. R: a language and environment for statistical computing. R Foundation for Statistical Computing, Vienna, Austria. https://www.R-project.org/.
69. Thevenot EA, Roux A, Xu Y, Ezan E, Junot C. 2015. Analysis of the human adult urinary metabolome variations with age, body mass index, and gender by implementing a comprehensive workflow for univariate and OPLS statistical analyses. J Proteome Res 14:3322–3335. https://doi.org/10.1021/acs.jproteome.5b00354.
70. Mock A, Warta R, Dettling S, Brors B, Jager D, Herold-Mende C. 2018. MetaboDiff: an R package for differential metabolomic analysis. Bioinformatics 34:3417–3418. https://doi.org/10.1093/bioinformatics/bty344.
71. Huber W, von Heydebreck A, Sultmann H, Poustka A, Vingron M. 2002. Variance stabilization applied to microarray data calibration and to the quantification of differential expression. Bioinformatics 18(Suppl 1):S96–S104. https://doi.org/10.1093/bioinformatics/18.suppl_1.s96.

Downloaded from https://journals.asm.org/journal/mbio on 08 September 2022 by 153.90.170.56.